Supplementary materials

Dimeric 1,3,5-triazinane-based derivatives as corrosion inhibitors for Q235 carbon steel in 1.0 mol·L^{-1} HCl

Yuan Wang[a], Wenwen Song[b], Wenhui Gong[c], Junbo Xu[b], Youwei Li[b], Qibin Chen*[c]

[a]*State Key Laboratory of Oil and Gas Equipment, Tubular Goods Research Institute of CNPC, Xi'an, Shanxi, 710077, P. R. China*

[b]*Tarim Oilfield Company, Petrochina, Korla, Xinjiang, 841000, P. R. China*

[c]*State Key Laboratory of Chemical Engineering and School of Chemistry & Molecular Engineering, East China University of Science and Technology, Shanghai, 200237, P. R. China*

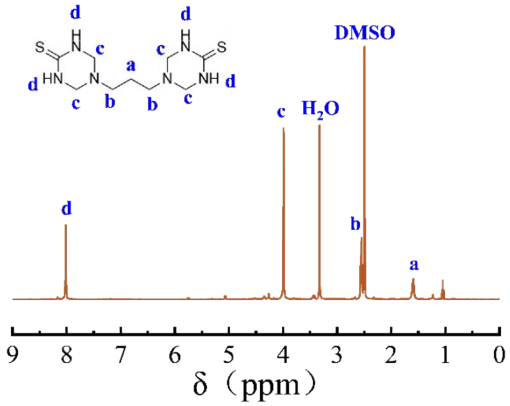

Figure S1. 1H NMR spectra of PBT.

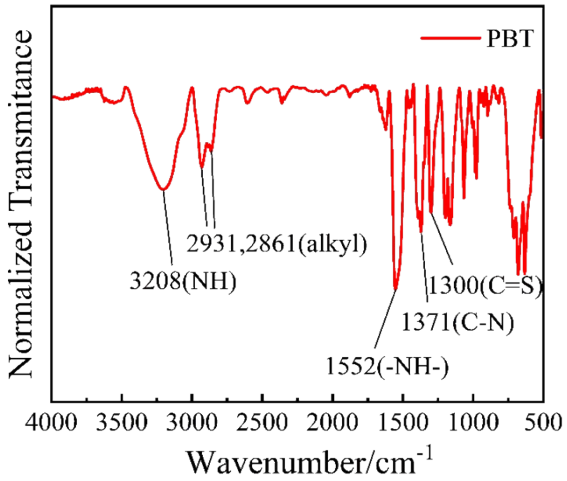

Figure S2. FT-IR spectra of PBT.

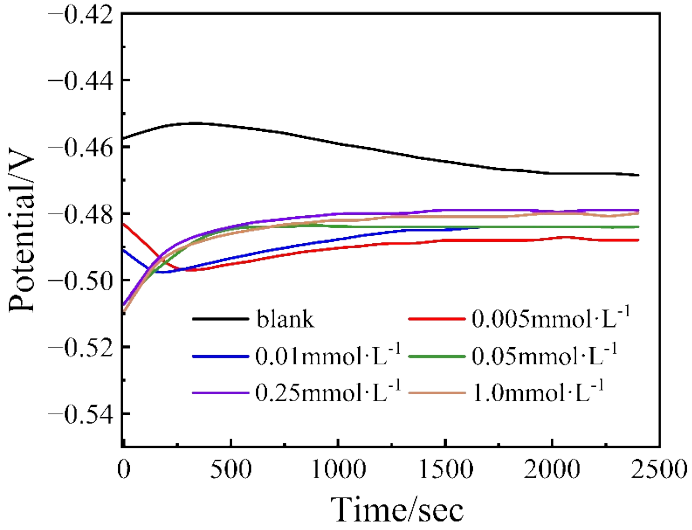

Figure S3. Open circuit potential versus time in 1.0 mol·L^{-1} HCl solution containing different concentrations of PBT.

In Figure S3, the variation of the open circuit potential in solution over time is shown. The E_{OCP} (subscript OCP is the open circuit potential) of Q235 CS rises slightly at first in the HCl solution, then moves to a more negative potential, and the E_{OCP} reaches a stable value after about 1800s of immersion, eventually stabilizing around -0.470 V. However, in inhibition solutions containing different concentrations of PBT, the time for E_{OCP} to reach stabilization gives a shorter time, which is related to the concentration of PBT. Overall, the E_{OCP}s in the experimental solutions does not change much at 2400s of the experimental time and can be considered to have reached their stabilization potentials, respectively[1].

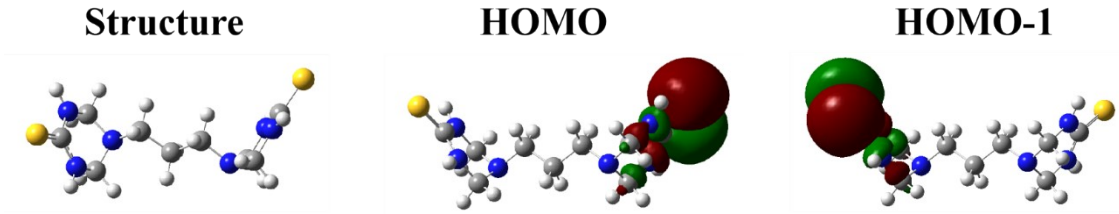

Figure S4. Optimized structures, HOMO and HOMO-1 of PBT.

Table S1. The results of the quantum chemical calculation for PBT.

Inhibitor	E_{HOMO}/eV	E_{HOMO-1}/eV	ΔE/eV
PBT	-5.4985	-5.4993	0.0008

Density functional theory (DFT) calculation formulae are given as follows:

$$I = -E_{HOMO} \quad (1)$$

$$A = -E_{LUMO} \tag{2}$$

$$\chi = \frac{I + A}{2} \tag{3}$$

$$\gamma = \frac{I - A}{2} \tag{4}$$

$$\Delta N = \frac{\chi_{Fe} - \chi_{int}}{2(\gamma_{Fe} + \gamma_{inh})} \tag{5}$$

Herein, the theoretical values χ_{Fe} = 7 eV·mol·L^{-1} and γ_{Fe} = 0 eV·mol·L^{-1}[2].

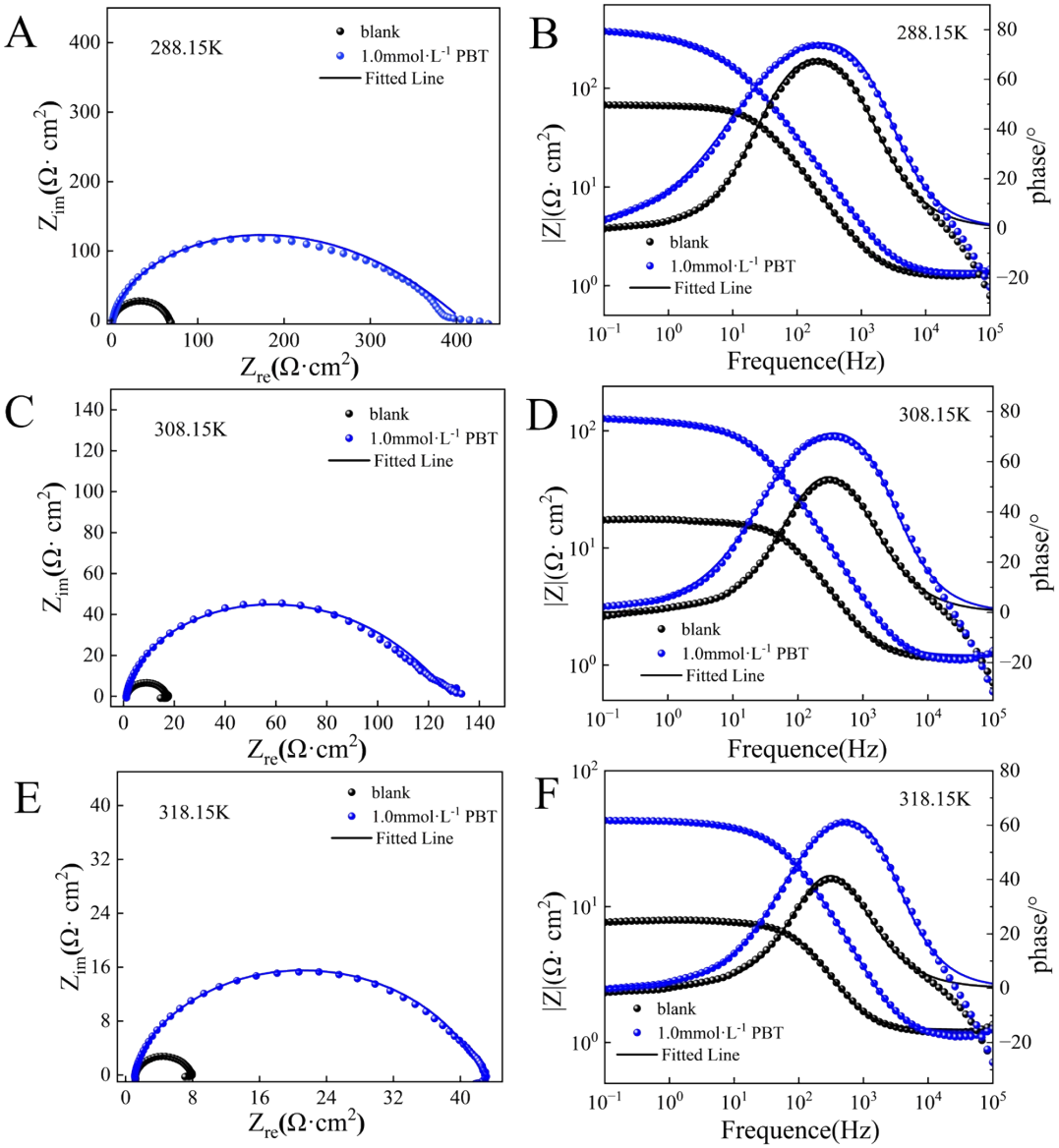

Figure S5 Nyquist plots (A, C and E) and Bode phase angle plots (B, D and F) for Q235 CS in 1.0 mol·L^{-1} HCl with 1.0 mmol L^{-1} of PBT at different temperature: 288.15K (A and B), 308.15K (C and D) and 318.15K (E and F).

Table S2. EIS parameters for Q235 CS in 1.0 mol·L^{-1} HCl with 1.0 mmol L^{-1} of PBT at 288.15, 308.15 and 318.15K.

T/K	C/ mmol·L^{-1}	R_S/Ω·cm^2	CPE_f		R_f	CPE_{dl}		R_{ct}	R_P	η
			Y_0/μΩ·S^n·cm^2	n_1		Y_0/μΩ·S^n·cm^2	n_2			
288.15K	blank	1.311				143.9	0.9295	65.48	65.48	
	1.0	1.405	39.02	1	8.835	33.82	0.5153	397.7	406.5	83.9%
308.15K	blank	1.190				242.7	0.9157	15.71	15.71	
	1.0	1.211	44.37	1	13.19	41.90	0.5246	115.3	128.5	87.8%
318.15K	blank	1.239				358.3	0.9221	6.465	6.465	
	1.0	1.188	46.06	1	10.63	48.09	0.6659	30.98	41.61	84.5%

Table S3. Comparison of inhibition behavior of reported triazine corrosion inhibitors with PBT synthesized in this work.

Inhibitor	Concentration	Media	IE(%)	Ref.
2,4-diphenyl-6-((1E)-1-(4-phenyl-2-(phenyldiazenyl) tetraaz-3-en-1-ylidene)ethyl)-2,3,4,5-tetrahydro-1,2,4-triazine	0.1mM	1M HNO_3	91.4%	[3]
2,4-diphenyl-6-((E)-1-((E)-4-phenyltetraaz-2-en-1-ylidene) ethyl)-2,3,4,5-tetrahydro-1,2,4-triazine			88.9%	
3-(4-thioxo-1,3,5-triazinan-1-yl) propanoic acid (TPA)	0.21mM	CO_2 saturated oilfield water	97.8%	[4]
1,5-diphenyl-1,3,5-triazinane-2- thione (DTT)			99.1%	
6-N,N-bis(6-methylheptyl)amine-1,3,5-triazine-2,4-dithiolmono-sodium, (*iso*-DON)	1.5mM	3.5 wt% NaCl	93.0%	[5]
6-dibutylamino-1,3,5-triazine-2,4-dithiol monosodium (DBN)			95.0%	
2-amino-4-methoxy-6-methyl-1,3,5-triazine	10.0mM	0.5 M HCl	95.7%	[6]
2-(n-Hexylamino)-4,6-bis (3-N, N-dimethylaminopropyl) amino-1,3,5-triazine	1.0mM	1.0 M HCl	93.45%	[7]

2-(n-Octylamino)-4,6-bis (3-N, N-dimethylaminopropyl) amino-1,3,5-triazine	94.41%
2-(n-n-Dodecylamino)-4,6-bis(3-N,N-dimethylaminopropyl) amino-1,3,5-triazine	96.66%

Reference

1 L. L. Liao, S. Mo, H. Q. Luo, Y. J. Feng, H. Y. Yin and N. B. Li, Corros. Sci. 2017, 124, 167-177.

2 J. T. Zhang, M. J. Kong, J. T. Feng, C. X. Yin, D. Q. Li, L. Fan, Q. B. Chen and H. L. Liu, J. Mol. Liq. 2021, 344, 117962.

3 K. Shalabi, E. Abdel-Galil, A. H. El-Askalany and Y. M. Abdallah, J. Mol. Liq. 2022, 348, 118420.

4 X. Wang, W. L. Xu, G. A. Zhang and Z. Y. Liu, Corros. Sci. 2023, 220, 111288.

5 Q. Zhao, R. H. Hou, X. L. Wang, S. Q. Tang, W. W. Zhao, X. B. Hu and H. Q. Li, Int. J. Electrochem. Sci. 18 (2023) 100285.

6 V. Ökten, R. Yildiz, G. Sigircik, Anti-Corros. Method M. 70 (2023) 350-360.

7 X. H. Jin, J. B. Wang, S. Y. Zheng, J. A. Li, X. M. Ma, L. Feng, H. L. Zhu and Z. Y. Hu , J. Mol. Liq. 353 (2022) 118747.